Article

Electrophysiological and Pupillometric Abnormalities in PROM1 Cone–Rod Dystrophy

Jason C. Park[1], Frederick T. Collison[2], Gerald A. Fishman[1,2], and J. Jason McAnany[1]

[1] Department of Ophthalmology and Visual Sciences, University of Illinois at Chicago, Chicago, IL, USA
[2] The Pangere Center for Inherited Retinal Diseases, The Chicago Lighthouse, Chicago, IL, USA

Purpose: To compare electrophysiological and pupillometric responses in subjects with cone–rod dystrophy due to autosomal recessive (AR) PROM1 mutations.

Methods: Four subjects with AR PROM1 dystrophy and 10 visually normal, age-similar controls participated in this study. Full-field, light- and dark-adapted electroretinograms (ERGs) were obtained using conventional techniques. Full-field, light- and dark-adapted measures of the pupillary light reflex (PLR; pupil constriction elicited by a flash of light) were obtained across a range of stimulus luminance using long- and short-wavelength light. Pupil size as a function of stimulus luminance was described using Naka–Rushton functions to derive P_{max} (maximum response) and s (pupil response sensitivity).

Results: Light-adapted ERGs were non-detectable in all four PROM1 subjects, whereas dark-adapted ERGs were non-detectable in three subjects and markedly attenuated in the fourth. By contrast, each PROM1 subject had light- and dark-adapted PLRs. P_{max} ranged from normal to slightly attenuated under all conditions. Light-adapted s was generally normal, with the exception of two subjects who had abnormal s for the long-wavelength stimulus. Dark adapted s was abnormal for each PROM1 subject for the long-wavelength stimulus and ranged from the upper limit of normal to substantially abnormal for the short-wavelength stimulus.

Conclusions: ERG and PLR comparison showed an unanticipated dichotomy: ERGs were generally non-detectable, whereas PLRs were normal for all PROM1 subjects under select conditions. Differences between the measures may be attributed to distinct spatiotemporal summation/gain characteristics.

Translational Relevance: These data highlight the potential usefulness of pupillometry in cases where the ERG is non-detectable.

Introduction

Mutations in the *PROM1* gene that encodes Prominin-1 result in retinal dystrophies. Prominin-1 is a transmembrane glycoprotein that localizes to the base of photoreceptor outer segments and is thought to be involved in disc assembly and maintenance of outer segment structure.[1,2] These dystrophies can be inherited in autosomal dominant (AD) or autosomal recessive (AR) forms. AD *PROM1* dystrophy tends to have a later onset and a milder phenotype compared to AR *PROM1* dystrophy.[3] To date, more than two dozen distinct pathogenic mutations in *PROM1* have been reported, with the vast majority associated with an AR mode of inheritance.[4]

AR mutations in *PROM1* produce severe phenotypes that have been described as cone–rod dystrophy,[5–7] retinitis pigmentosa with macular involvement,[8,9] or Leber congenital amaurosis.[10] High myopia and visual dysfunction are characteristically apparent early in life.[6,11] Retinal dysfunction, including markedly reduced or non-detectable full-field electroretinograms (ERGs), is common by 30 years of age.[1,6,8,9,12] A recent report of four individuals having AR *PROM1* mutations showed that several clinical characteristics were common among them.[13] Specifically, oval-shaped macular lesions were observed on fundus examination, and small, circular, hypoautofluorescent lesions within the posterior pole were apparent by near-infrared autofluorescence. In addition, their light-adapted ERGs were markedly reduced or

1

non-detectable, the dark-adapted mixed rod–cone ERG a-wave was nearly absent, and the b-wave was substantially reduced in amplitude and had delayed implicit time.

Given that the ERGs are non-detectable or severely attenuated, electrophysiological assessment is not likely to be a useful approach for monitoring retinal function in adult individuals who have AR *PROM1* mutations. As such, non-invasive, objective approaches to assess visual function in these individuals that could serve as future outcome measures in clinical trials are lacking. Recently, our group[14–17] and others[18–20] have explored the use of pupillometry as a functional measure in individuals who have inherited retinal degenerative diseases and functional abnormalities. The pupillary light reflex (PLR), which is the response of the pupil to a flash of light, has not been reported in AR *PROM1* dystrophy, but this non-invasive, objective measure may be useful for assessing function in these individuals. PLR measurement has parallels to ERG recording in that it can be measured under dark- and light-adapted conditions to target rod- and cone-pathway function. Importantly, the PLR can be detectable in certain individuals who have inherited retinal dystrophies and no measurable full-field ERG.[19–22]

The purpose of the present study was to evaluate the usefulness of pupillometry as a potential outcome measure for future AR *PROM1* dystrophy clinical trials by recording and comparing the ERG and PLR measured with full-field stimuli under rod- and cone-mediated conditions. The ERG and PLR measurements were performed across a broad range of stimulus luminance to gain a better understanding of how the extent of abnormality varies for different stimuli. In addition, the post-illumination pupil response (PIPR) was assessed to provide a more direct measure of inner-retina function. The PIPR is believed to be generated by activation of the melanopsin photopigment that is contained within intrinsically photosensitive retinal ganglion cells (ipRGCs), largely independent of rod and cone photoreceptor contributions.[21,23–25] Thus, we sought to provide a comprehensive functional analysis in AR *PROM1* dystrophy.

Methods

Subjects

The research was approved by institutional review boards at the University of Illinois at Chicago and the Western IRB. The tenets of the Declaration of Helsinki were followed, and all subjects provided written informed consent prior to participating. Four
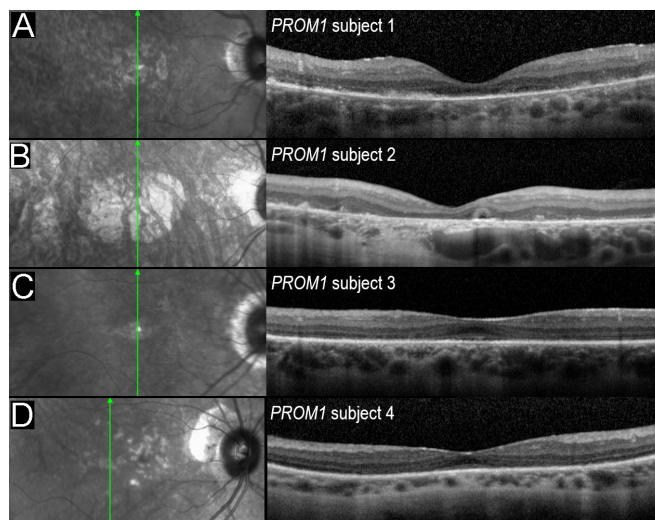

Figure 1. SLO images and OCT b-scans are shown for *PROM1* subject 1 (**A**), subject 2 (**B**), subject 3 (**C**), and subject 4 (**D**). The vertical *green line* on the SLO image shows the location of the corresponding OCT b-scan.

subjects (three males and one female; ages 27–35 years) with molecularly confirmed AR *PROM1* dystrophy were recruited from the cohort of the Pangere Center for Inherited Retinal Diseases at the Chicago Lighthouse. Two subjects were brothers, whereas the other subjects were unrelated. The clinical characteristics of these four individuals are detailed in a previous report.[13] The Table lists the sex, age, visual acuity, and molecular variants for the *PROM1* dystrophy subjects. Optical coherence tomography (OCT) b-scans and corresponding scanning laser ophthalmoscopy (SLO) images that demonstrate the location of each b-scan (vertical green line) are shown in Figure 1. These images are presented to provide an overview of the extent of structural abnormalities within the macula for each of the *PROM1* dystrophy subjects. Of note, the OCT images for *PROM1* subjects 1 and 4 were obtained on the date that the ERG and pupil measures were obtained, whereas the images for *PROM1* subjects 2 and 3 were obtained 3 years and 1 year prior to the present study, respectively. Each of the four *PROM1* dystrophy subjects had marked structural abnormalities. *PROM1* subject 1 had inner segment ellipsoid (ISe) band loss throughout the scan but some preservation of the outer nuclear layer (ONL) at the fovea. *PROM1* subject 2 had loss of the ISe and reduced ONL throughout the scan, as well as thinning of the retinal pigment epithelium at the fovea; an outer-retinal tubulation was apparent parafoveally. *PROM1* subjects 3 and 4 generally lacked the ISe, except at the fovea, where it appeared thin and hyporeflective; there was some preservation of the ONL throughout the scan.

Table. Subject characteristics

Subject	Sex	Age (y)	Visual Acuity (logMAR)	*PROM1* Variant	Amino Acid Change
1	Male	27	1.20	c.1157T>A	p.Leu386*
				c.1557C>A	p.Tyr519*
2	Male	35	1.35	c.1182_1202del	p.Asn395_Pro401del
				chr4:16017462_16024802del	Deletion of 2 exons
3	Male	29	0.64	c.1182_1202del	p.Asn395_Pro401del
				chr4:16017462_16024802del	Deletion of 2 exons
4	Female	33	1.02	c.1274+2T>C	Affects splicing
				c.2077-521A>G	Affects splicing

Ten visually normal control subjects (five males and five females; ages 24–41 years) with no history of eye disease also participated in the study. The control subjects had Early Treatment of Diabetic Retinopathy Study best-corrected visual acuity of 0 logarithm of the minimum angle of resolution (logMAR) or better and normal contrast sensitivity assessed with the Pelli–Robson chart. An independent samples *t*-test indicated that the mean age of the controls (30.1 years) did not differ significantly ($t = 0.36$, $P = 0.73$) from that of the *PROM1* dystrophy subjects (31.0 years).

ERG Measurement

ERGs were recorded using DTL corneal electrodes that were referenced to the ear using a gold-cup electrode. A gold-cup electrode also served as the ground (forehead). Amplifier bandpass settings were 0.30 to 500 Hz, and the sampling frequency was 2 kHz. Following adaptation to a uniform achromatic field (30 cd/m^2), light-adapted responses were elicited by light-emitting diode (LED)-generated achromatic 3.0 cd·s/m^2 flashes (4 ms) and flicker (31.25 Hz) stimuli. Subjects were then dark-adapted for 20 minutes, and responses were elicited by LED-generated achromatic flashes (4 ms) that ranged from 0.0001 to 10.0 cd·s/m^2. All stimuli were generated by and presented in a Color-Dome ganzfeld and responses were acquired with an Espion E^3 electrophysiology system (Diagnosys LLC, Lowell, MA). For each stimulus luminance, a minimum of three responses were obtained and averaged for analysis.

Pupil Measurements

Each subject underwent full-field pupillometry recording, using methods that have been described elsewhere.[15] In brief, subjects were dark adapted for 10 minutes, and the responses of the pupil to flashes (1 second) of long-wavelength (642 nm) light and short-wavelength (465 nm) light were recorded using an infrared videography system (Arrington Research, Inc. Scottsdale, AZ). Stimulus luminance ranged from 0.0001 to 450 cd/m^2. Following the dark-adapted measurements, the subjects were light adapted for 2 minutes to a 6-cd/m^2 short-wavelength (465 nm) field. The responses of the pupil to flashes (1 second) of long-wavelength (642 nm) light and short-wavelength (465 nm) light presented against this field were recorded, with stimulus luminance ranging from 0.1 to 450 cd/m^2. All stimuli were generated by and presented in a ColorDome ganzfeld (Diagnosys LLC). A minimum of two responses for each stimulus luminance were obtained and averaged for analysis. To minimize the effects of inter-subject differences in baseline pupil size, pupil diameter was normalized by the mean baseline pupil size during the 1 second preceding the flash. The transient PLR amplitude was defined as the difference between the normalized baseline diameter and the maximum pupil constriction following the stimulus onset.

For analysis, the transient PLR amplitude was plotted as a function of log stimulus luminance, and the data were fit with the following form of a Naka–Rushton function[26] to determine P_{max} (the maximum saturated PLR amplitude) and s (the PLR semi-saturation constant):

$$PLR = P_{max}\lceil L^n/(L^n + S^n)\rceil \qquad (1)$$

where L is the stimulus luminance, and n is the slope of the function. The value of n was set to 0.43 (mean of the control subjects), and P_{max} and s were determined by minimizing the mean squared error between the data and the fit ($1/s$ is a measure of pupil response sensitivity). Setting n to a constant value requires the assumption that the slope of the function relating PLR amplitude and log flash luminance is similar for all subjects. Limiting the number of free parameters was

necessary because, as shown below, some subjects had relatively few data points under light-adapted conditions that could be included in the fit. Limiting the fit to two free parameters helped to minimize overfitting the data.

In addition to assessing the transient PLR, we obtained a measure of the sustained pupil response, the PIPR. As discussed elsewhere,[21,23,24] the PIPR is a sustained pupillary constriction that is typically elicited by a high-luminance, short-wavelength stimulus. This response component is thought to be mediated by activation of the melanopsin photopigment that is contained in ipRGCs.[24,27] In the present study, a 450-cd/m^2 short-wavelength flash was used to elicit the PIPR, and the response was defined as the median pupil size from 5 to 7 seconds following the flash (6–8 seconds after the 1-second flash onset).

Statistical Analysis

Normality of the P_{max} and log s distributions was evaluated using the Shapiro–Wilk test. Both distributions were found to be normally distributed (both $P \geq 0.17$). Variance in the P_{max} and log s datasets for the *PROM1* dystrophy and control groups was evaluated using the Levene test for equality of variance. Variance within the two subject groups was found to be equivalent for both measures (both $P \geq 0.17$). Given the data distributions, differences between the two subject groups in log s and P_{max} were evaluated using two-way, repeated-measures analysis of variance (ANOVA). In these analyses, subject group (control vs. *PROM1* dystrophy) and condition (light-adapted, dark-adapted, long-wavelength, and short-wavelength) were included as main effects. Holm–Sidak pairwise comparisons were performed when appropriate.

Results

ERG Data

Figure 2 shows the mean dark-adapted ERG waveforms for the 10 control subjects (left column) and for the only *PROM1* dystrophy subject who had a detectable ERG (subject 4; right column). The other 3 *PROM1* dystrophy subjects had non-detectable dark-adapted responses, and no *PROM1* dystrophy subject had a detectable light-adapted response (data not shown). For the three lowest flash luminance levels (–4.0 to –2.0 log cd·s/m^2), a rod-pathway-driven b-wave was apparent in the mean control response but not in the responses of *PROM1* subject 4. With increasing flash luminance, the b-wave of the control group
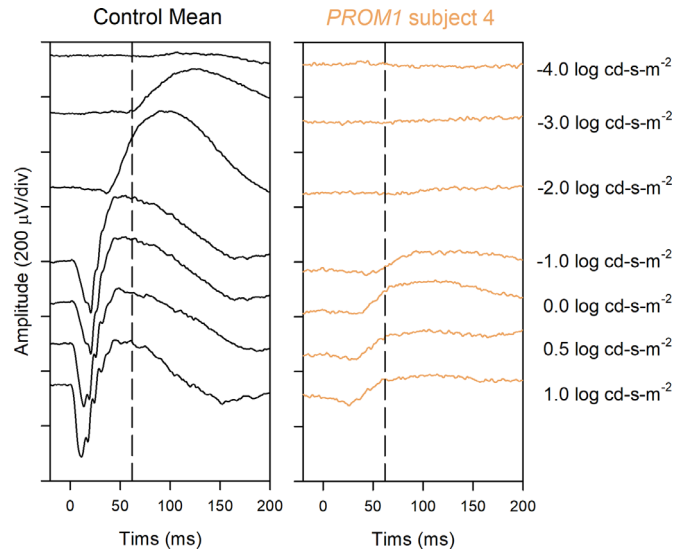

Figure 2. ERG waveforms obtained under dark-adapted conditions are shown for the control group (mean; *left*) and *PROM1* subject 4 (the only *PROM1* dystrophy subject who had detectable ERGs). Stimulus luminance is shown to the *right*, and the *vertical dashed lines* mark the onset of the b-wave for the lowest stimulus luminance that elicited a measurable response (the vertical line is replotted over the waveforms of *PROM1* subject 4 to aid timing comparisons).

increased in amplitude and occurred earlier in time, as expected.[28] The vertical dashed line marks the onset of the b-wave for the lowest flash luminance that reliably elicited a control response (–3.0 cd·s/m^2). For higher flash luminance levels, an a-wave became apparent for the controls (approximately –1.0 log cd·s/m^2 and higher). *PROM1* subject 4 had a somewhat unusual pattern for the higher flash luminance levels, as little or no a-wave was apparent, and the b-wave was attenuated and delayed. Indeed, the waveform shape for *PROM1* dystrophy subject 4 elicited by high-luminance flashes (0.0 to 1.0 log cd·s/m^2) resembled that of the control group recorded with a –3.0 log cd·s/m^2 flash, but the amplitude was reduced.

PLR Data

Figure 3 shows PLR amplitude as a function of log stimulus luminance for the controls (shaded area is the range of the control response) and each *PROM1* dystrophy subject. Individual *PROM1* dystrophy subject data are color coded, and the solid lines are fits of Equation 1 to the data. Responses obtained under the four conditions described above are shown. In general, each *PROM1* dystrophy subject generated PLRs under light- and dark-adapted conditions across most of the stimulus luminance range evaluated. For the long-wavelength stimulus under dark-adapted conditions (Fig. 3A), each *PROM1* dystrophy
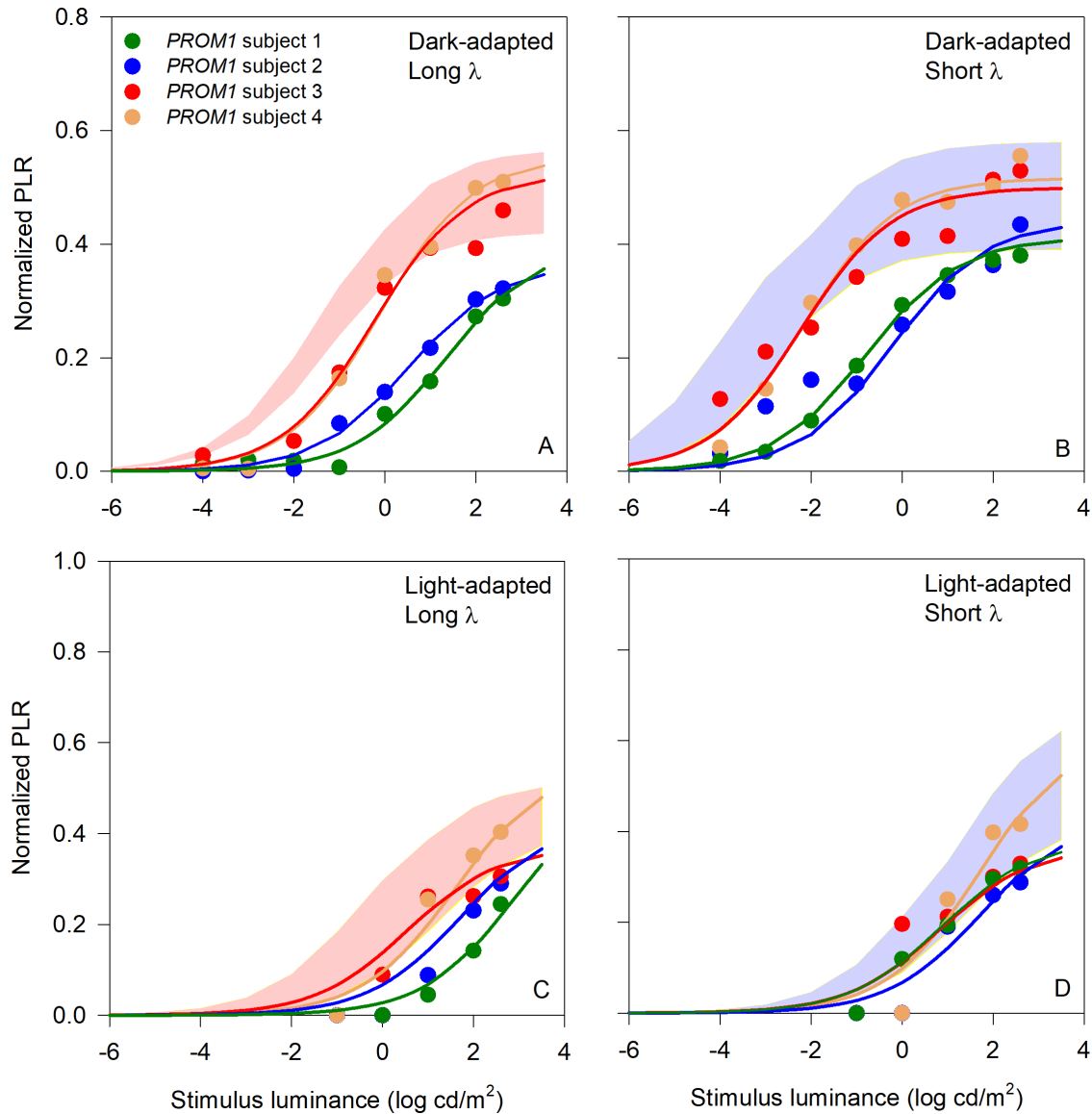
Figure 3. PLR amplitude is plotted as a function of log stimulus luminance measured under four conditions: (**A**) dark-adapted long-wavelength stimulus, (**B**) dark-adapted short-wavelength stimulus, (**C**) light-adapted long-wavelength stimulus, and (**D**) light-adapted short-wavelength stimulus. In each panel, the range (minimum to maximum) for the control group is indicated by the *shaded areas*, and the data for each *PROM1* dystrophy subject are indicated by the color-coded symbols.

subject had a reduced PLR for low to moderate stimulus luminance levels, whereas the PLRs for the highest flash luminance levels approached normal (subjects 1 and 2) or were normal (subjects 3 and 4). For the short-wavelength stimulus under dark-adapted conditions (Fig. 3B), subjects 1 and 2 had reduced PLRs for low to moderate stimulus luminance levels and nearly normal PLRs for the highest flash luminance levels. Subjects 3 and 4 tended to be at the lower limit of normal for low to moderate stimulus luminance levels and were well within the normal range for the highest flash luminance. The PLRs were generally normal,

or nearly normal, for the *PROM1* dystrophy subjects under light-adapted conditions (Figs. 3C, 3D) for high-luminance flashes. No *PROM1* dystrophy subject had a measurable PLR for the lowest luminance flash under light-adapted conditions, but the responses for the control subjects were also small.

The values of P_{max} derived from Equation 1 are shown in Figure 4 for the four conditions shown in Figure 3. The control subjects are represented by the open symbols, whereas the *PROM1* dystrophy subjects are color coded, as in Figure 3. In general, P_{max} was within the range of normal or only slightly reduced.
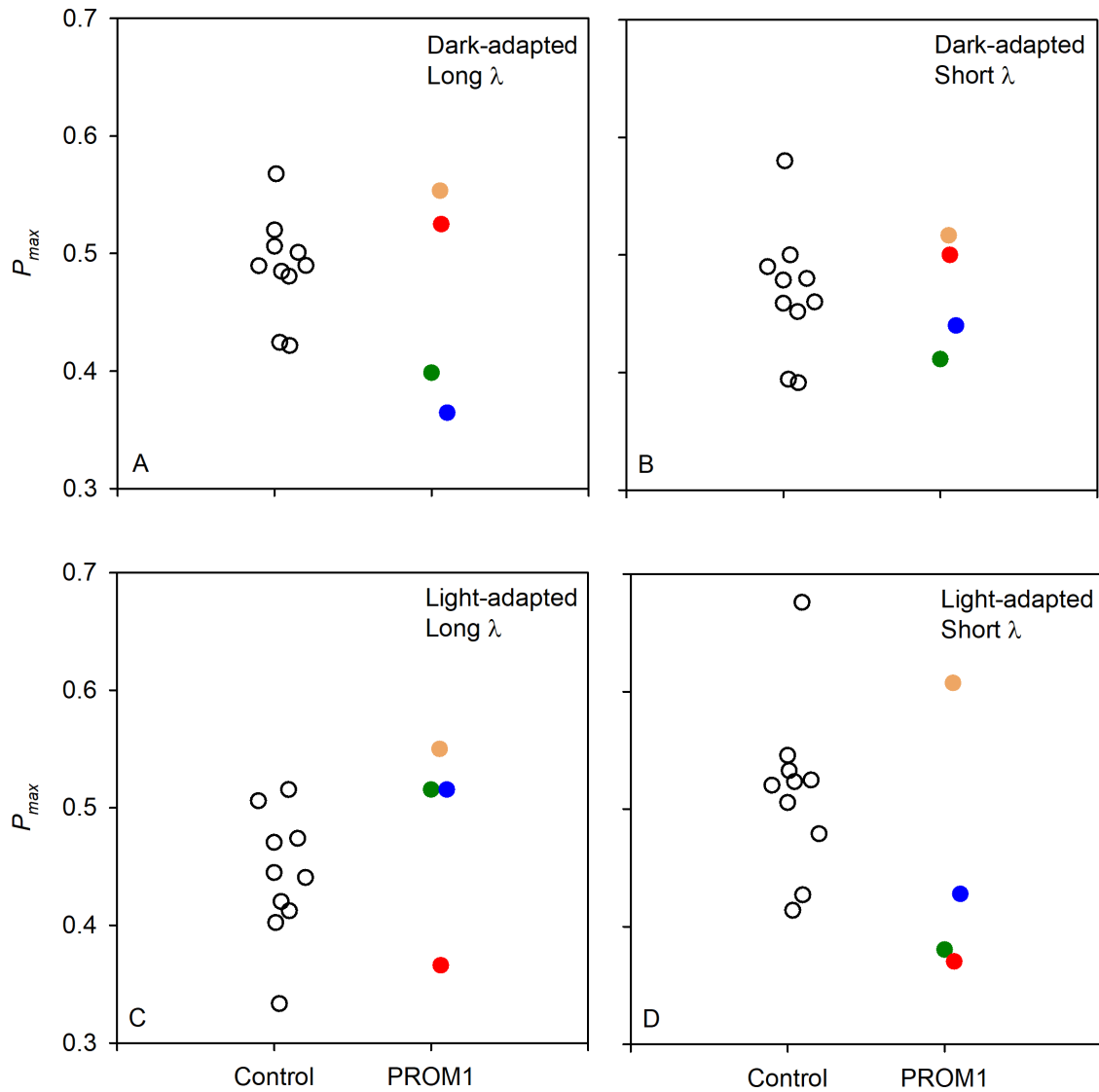
Figure 4. P_{max} is shown for the four conditions: (**A**) dark-adapted long-wavelength stimulus, (**B**) dark-adapted short-wavelength stimulus, (**C**) light-adapted long-wavelength stimulus, and (**D**) light-adapted short-wavelength stimulus. In each panel, the control subjects are indicated by the *open circles*, and the data for the *PROM1* dystrophy subjects are indicated by the color-coded symbols.

Specifically, P_{max} was slightly reduced for patients 1 and 2 under dark-adapted conditions for the long-wavelength stimulus (Fig. 4A). Under light-adapted conditions, subjects 1 and 3 had small decreases in P_{max} for the short-wavelength stimulus (Fig. 4D). However, these reductions were nominal; under no condition was P_{max} reduced by more than 6% from the lower limit of normal. ANOVA indicated no significant differences between the two subject groups ($F = 0.21$, $P = 0.66$) or among the four conditions ($F = 0.24$, $P = 0.87$) for P_{max}.

The values of log s derived from Equation 1 are shown in Figure 5 for the four conditions in the same format as that of Figure 4. In contrast

to P_{max}, log s was abnormal under dark-adapted conditions. Specifically, log s was increased (reduced sensitivity) for all four *PROM1* dystrophy subjects for both the long-wavelength stimulus (Fig. 5A) and the short-wavelength stimulus (Fig. 5B). Under light-adapted conditions, subjects 1, 2, and 3 had increased log s for the long-wavelength stimulus (Fig. 5C), whereas all four *PROM1* dystrophy subjects were within the normal range for the short-wavelength stimulus (Fig. 5D). ANOVA indicated significant differences between the two subject groups ($F = 22.76$, $P < 0.001$) and among the four conditions ($F = 158.64$, $P < 0.001$) for log s. The interaction between subject group and condition was also significant ($F = 8.39$,
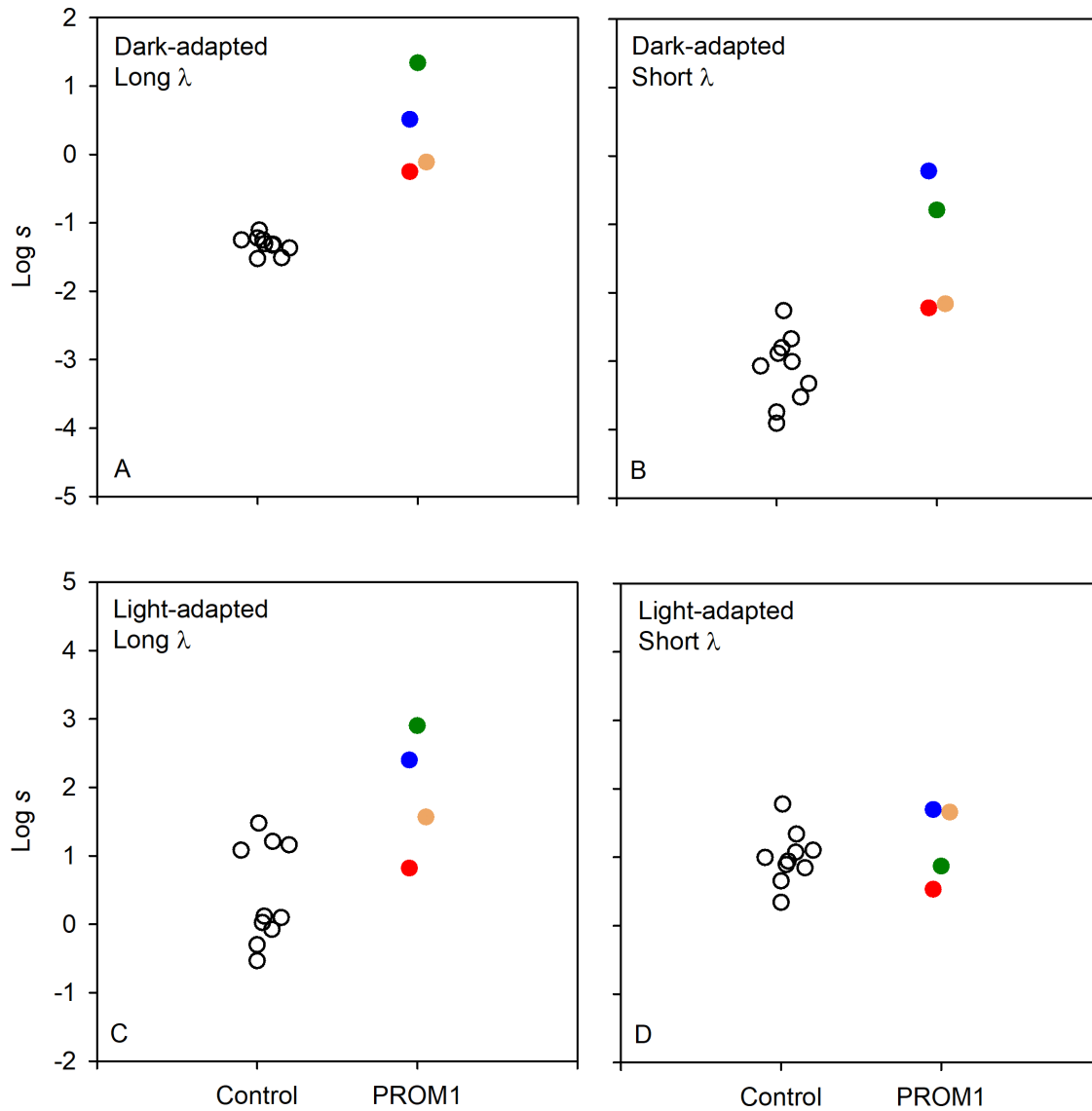
Figure 5. Log *s* is shown for the four conditions; all other conventions are like those of Figure 4.

$P < 0.001$). Holm–Sidak pairwise comparisons indicated significant differences between the subject groups for all conditions (all $t > 2.28$, $P < 0.001$), with the exception of the light-adapted short-wavelength condition ($t = 0.55$, $P = 0.58$) (Fig. 5D).

Figure 6 shows normalized pupil size over time for the highest luminance (450 cd/m²) short-wavelength (top) and long-wavelength (bottom) flash. The normal control ranges are indicated by the gray areas, and the pupil size over time for each *PROM1* dystrophy subject is indicated by the color-coded traces. For the short-wavelength flash, the initial transient constriction was within the normal range for subjects 2, 3, and 4, and was slightly reduced for subject 1.

Likewise, the sustained component of the response (measured over the 5- to 7-second window from flash offset; dashed lines) was within the range of normal for subjects 2, 3, and 4, and was slightly reduced for subject 1. However, this slight reduction for subject 1 can likely be attributed to the small reduction in the rod/cone-mediated transient component. For the long-wavelength flash (bottom), the initial transient constriction was within the normal range for all subjects. Of note, little sustained component was elicited by the long-wavelength flash for either subject group, as expected. In summary, the sustained (melanopsin-mediated) component of the response elicited by the short-wavelength flash was generally normal for all four *PROM1* dystrophy subjects.
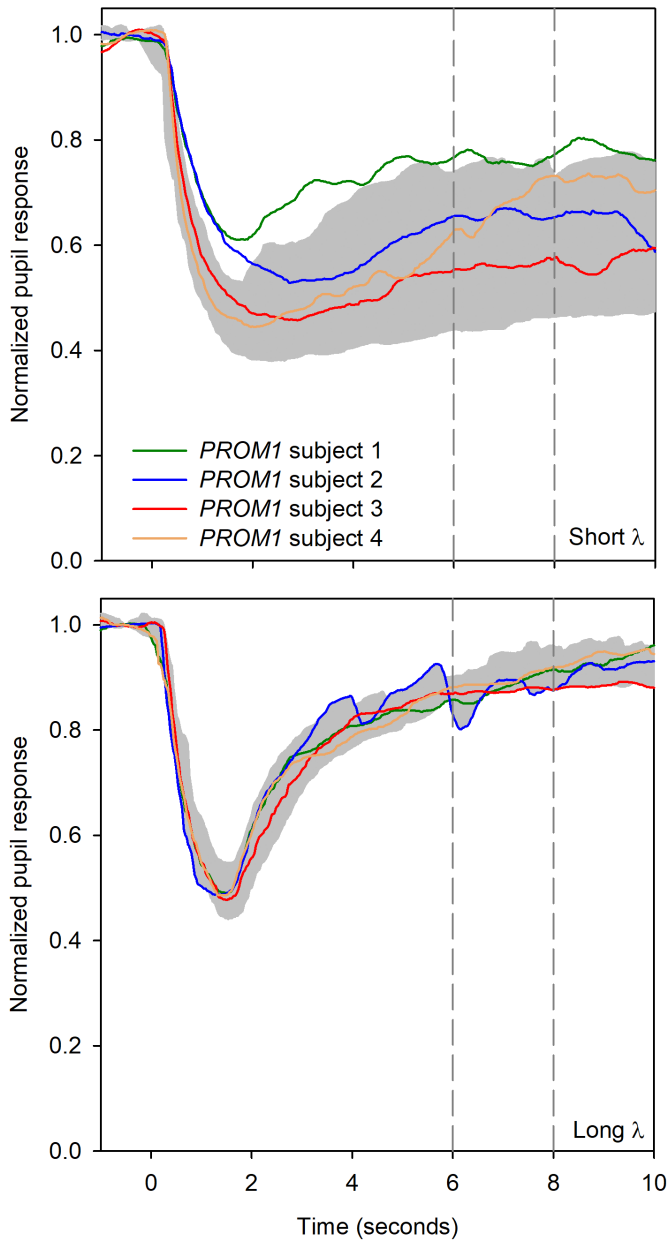
Figure 6. Pupil size over time following 1-second 450-cd/m² flashes of short-wavelength light (*top*) and long-wavelength light (*bottom*). The *gray regions* mark the normal control range (minimum to maximum), and the color-coded traces represent the pupil response for each *PROM1* dystrophy subject. The PIPR was measured 5 to 7 seconds after the offset of the stimulus (6 to 8 seconds after stimulus onset) as indicated by the *vertical dashed lines*.

Discussion

This study evaluated full-field ERG and PLR measures of function in subjects who have AR *PROM1* dystrophy. The present dataset shows profound ERG abnormalities in these individuals, consistent with the literature.[1,6,8,9,12] Specifically, three of the

four *PROM1* dystrophy subjects had no measurable light- or dark-adapted ERGs. For one subject (*PROM1* subject 4), the ERG was measurable under dark-adapted conditions for high-luminance stimuli. However, this subject's waveform for high-luminance stimuli resembled that of the normal control response obtained with low-luminance stimuli. Specifically, the a-wave was absent and the b-wave was characterized by a slow, delayed response. This response pattern may be explained by a marked sensitivity loss (approximately $100\times$ to $1000\times$ less sensitive than normal). That is, the response of *PROM1* subject 4 is like that of a control subject viewing the stimulus through a dark filter (e.g., 2 to 3 log unit neutral-density filter). In addition, this subject may have a reduced maximum saturated b-wave amplitude, such that no flash luminance would be sufficient to elicit a normal response. Taken together, the complete absence of the full-field ERG in three of the four subjects indicates that this may not be a particularly useful approach for subtyping these individuals or for monitoring retinal function in therapeutic trials involving adult subjects. We note, however, that each of the four subjects had markedly reduced, but detectable, dark-adapted ERGs earlier in life (ages 4 to 21 years).

The pattern of pupillometry data differed substantially from that of the ERG data. Whereas the adult *PROM1* dystrophy subjects had non-detectable or markedly impaired ERGs, they all had measureable PLRs that were normal under certain conditions. For example, for the short-wavelength stimulus presented under light-adapted conditions, the PLRs of all subjects were normal or nearly normal. For the long-wavelength stimulus presented under light-adapted conditions, the PLRs of subjects 3 and 4 were normal, whereas subjects 1 and 2 showed sensitivity losses. The apparent discrepancy between the absent light-adapted ERGs and the generally robust light-adapted PLRs is likely due to differences in the spatial summation characteristics of these two measures. We have shown previously that a small area of normal cone function (e.g., diameter subtending 4° of visual angle) may be sufficient to drive a normal full-field, cone-mediated pupil response.[17] In contrast, the cone-pathway-mediated ERG is highly dependent on spatial summation of the response, as a small region of residual cone photoreceptors will not produce a normal full-field ERG. Evidence for residual cone photoreceptor function comes from a previous study that showed measurable, although abnormal, multifocal ERGs in a *PROM1* dystrophy subject who had little or no measurable light-adapted full-field ERGs.[7] Thus, there may be regions of functional cone photoreceptors, at least in some *PROM1* dystrophy subjects, which could explain

the nearly normal PLRs that were obtained under light-adapted conditions. Multifocal chromatic pupillometry[18,29,30] may provide an additional tool to better understand rod- and cone-mediated pupil responses and their spatial summation characteristics, elicited throughout different areas of the visual field in *PROM1* dystrophy.

PLRs were also measurable for each *PROM1* dystrophy subject under dark-adapted conditions, but these responses were not necessarily normal. The marked sensitivity loss at the photoreceptor level, as indicated by the dark-adapted ERG, appears to manifest as a sensitivity loss in the dark-adapted pupil response. This can be seen as a rightward shift of the pupil datasets in Figures 3A and 3B, as well as in the measurements of pupil log *s* (Figs. 5A, 5B). The rod-mediated PLR exhibits spatial summation across a large retinal area, which is unlike the spatial summation properties of the cone-mediated PLR.[17] Thus, a small residual area of rod function is not expected to generate a normal rod-mediated PLR. Interestingly, the transient and sustained components of the pupil response for the dark-adapted, short-wavelength, high-luminance stimulus were generally normal for all four *PROM1* dystrophy subjects (Fig. 6). This suggests preserved inner-retina function and that the visual signal is transmitted through the pupil pathway, at least under this condition. This conclusion is supported by normal flash visually evoked potentials that were reported in a *PROM1* dystrophy subject who had substantially impaired full-field ERGs.[7] Thus, despite the profound photoreceptor impairment that is apparent by ERG, the visual pathway of certain *PROM1* dystrophy subjects may remain at least partially intact, which provides hope for future therapeutic efforts.

There are a few important considerations for interpreting the results of the present report. First, the sample size is small, given that *PROM1* mutations have a low prevalence in the population. Nevertheless, the pattern of results was generally similar for the four subjects. An additional consideration is that the Naka–Rushton fits to the PLR data under light-adapted conditions contained relatively few data points. The values of log *s* and P_{max} may be better defined by including a finer sampling of stimulus luminance and extending the maximum stimulus luminance beyond 450 cd/m^2. Including a finer sampling of stimulus luminance may also provide sufficient data to evaluate the slope of the Naka–Rushton function, which was assumed to be constant in the preset report.

In summary, we provide evidence that the response of the pupil to flashes of light can be measured in some adult AR *PROM1* subjects who have little or no ERG responses. Differences between the ERG and PLR may be attributed to residual photoreceptor function and spatiotemporal summation/gain differences between these measures. These data highlight the potential usefulness of pupillometry in cases where the ERG is non-detectable and suggest that the PLR may be a useful measure for subtyping and following *PROM1* dystrophy subjects in future clinical trials and in natural history studies.

References

1. Maw MA, Corbeil D, Koch J, et al. A frameshift mutation in prominin (mouse)-like 1 causes human retinal degeneration. *Hum Mol Genet*. 2000;9:27–34.
2. Lu Z, Hu X, Reilly J, et al. Deletion of the transmembrane protein Prom1b in zebrafish disrupts outer-segment morphogenesis and causes photoreceptor degeneration. *J Biol Chem*. 2019;294:13953–13963.
3. Michaelides M, Gaillard MC, Escher P, et al. The *PROM1* mutation p.R373C causes an autosomal dominant bull's eye maculopathy associated with rod, rod-cone, and macular dystrophy. *Invest Ophthalmol Vis Sci*. 2010;51:4771–4780.
4. Liang J, She X, Chen J, et al. Identification of novel *PROM1* mutations responsible for autosomal recessive maculopathy with rod-cone dystrophy. *Graefes Arch Clin Exp Ophthalmol*. 2019;257:619–628.
5. Pras E, Abu A, Rotenstreich Y, et al. Cone-rod dystrophy and a frameshift mutation in the *PROM1* gene. *Mol Vis*. 2009;15:1709–1716.
6. Khan AO, Bolz HJ. Pediatric cone-rod dystrophy with high myopia and nystagmus suggests

recessive *PROM1* mutations. *Ophthalmic Genet.* 2015;36:349–352.

7. Eidinger O, Leibu R, Newman H, Rizel L, Perlman I, Ben-Yosef T. An intronic deletion in the *PROM1* gene leads to autosomal recessive cone-rod dystrophy. *Mol Vis.* 2015;21:1295–1306.

8. Zhang Q, Zulfiqar F, Xiao X, et al. Severe retinitis pigmentosa mapped to 4p15 and associated with a novel mutation in the *PROM1* gene. *Hum Genet.* 2007;122:293–299.

9. Permanyer J, Navarro R, Friedman J, et al. Autosomal recessive retinitis pigmentosa with early macular affectation caused by premature truncation in *PROM1*. *Invest Ophthalmol Vis Sci.* 2010;51:2656–2663.

10. Ragi SD, Lima de Carvalho JR, Jr, Tanaka AJ, et al. Compound heterozygous novel frameshift variants in the *PROM1* gene result in Leber congenital amaurosis. *Cold Spring Harb Mol Case Stud.* 2019;5:a004481.

11. Cehajic-Kapetanovic J, Birtel J, McClements ME, et al. Clinical and molecular characterization of *PROM1*-related retinal degeneration. *JAMA Netw Open.* 2019;2:e195752.

12. Littink KW, Koenekoop RK, van den Born LI, et al. Homozygosity mapping in patients with cone-rod dystrophy: novel mutations and clinical characterizations. *Invest Ophthalmol Vis Sci.* 2010;51:5943–5951.

13. Collison FT, Fishman GA, Nagasaki T, et al. Characteristic ocular features in cases of autosomal recessive PROM1 cone-rod dystrophy. *Invest Ophthalmol Vis Sci.* 2019;60:2347–2356.

14. Collison FT, Park JC, Fishman GA, Stone EM, McAnany JJ. Two-color pupillometry in enhanced S-cone syndrome caused by NR2E3 mutations. *Doc Ophthalmol.* 2016;132:157–166.

15. Collison FT, Park JC, Fishman GA, Stone EM, McAnany JJ. Two-color pupillometry in KCNV2 retinopathy. *Doc Ophthalmol.* 2019;139:11–20.

16. Collison FT, Park JC, Fishman GA, McAnany JJ, Stone EM. Full-field pupillary light responses, luminance thresholds, and light discomfort thresholds in CEP290 Leber congenital amaurosis patients. *Invest Ophthalmol Vis Sci.* 2015;56:7130–7136.

17. Park JC, McAnany JJ. Effect of stimulus size and luminance on the rod-, cone-, and melanopsin-mediated pupillary light reflex. *J Vis.* 2015;15:13.

18. Ben Ner D, Sher I, Hamburg A, et al. Chromatic pupilloperimetry for objective diagnosis of Best vitelliform macular dystrophy. *Clin Ophthalmol.* 2019;13:465–475.

19. Kawasaki A, Crippa SV, Kardon R, Leon L, Hamel C. Characterization of pupil responses to blue and red light stimuli in autosomal dominant retinitis pigmentosa due to NR2E3 mutation. *Invest Ophthalmol Vis Sci.* 2012;53:5562–5569.

20. Krishnan AK, Jacobson SG, Roman AJ, et al. Transient pupillary light reflex in CEP290- or NPHP5-associated Leber congenital amaurosis: latency as a potential outcome measure of cone function. *Vision Res.* 2020;168:53–63.

21. Park JC, Moura AL, Raza AS, Rhee DW, Kardon RH, Hood DC. Toward a clinical protocol for assessing rod, cone, and melanopsin contributions to the human pupil response. *Invest Ophthalmol Vis Sci.* 2011;52:6624–6635.

22. Kardon R, Anderson SC, Damarjian TG, Grace EM, Stone E, Kawasaki A. Chromatic pupillometry in patients with retinitis pigmentosa. *Ophthalmology.* 2011;118:376–381.

23. Kelbsch C, Strasser T, Chen Y, et al. Standards in pupillography. *Front Neurol.* 2019;10:129.

24. Gamlin PD, McDougal DH, Pokorny J, Smith VC, Yau KW, Dacey DM. Human and macaque pupil responses driven by melanopsin-containing retinal ganglion cells. *Vision Res.* 2007;47:946–954.

25. Kardon R, Anderson SC, Damarjian TG, Grace EM, Stone E, Kawasaki A. Chromatic pupil responses: preferential activation of the melanopsin-mediated versus outer photoreceptor-mediated pupil light reflex. *Ophthalmology.* 2009;116:1564–1573.

26. McCulloch DL, Kondo M, Hamilton R, et al. ISCEV extended protocol for the stimulus-response series for light-adapted full-field ERG. *Doc Ophthalmol.* 2019;138:205–215.

27. Dacey DM, Liao HW, Peterson BB, et al. Melanopsin-expressing ganglion cells in primate retina signal colour and irradiance and project to the LGN. *Nature.* 2005;433:749–754.

28. McCulloch DL, Marmor MF, Brigell MG, et al. ISCEV Standard for full-field clinical electroretinography (2015 update). *Doc Ophthalmol.* 2015;130:1–12.

29. Chibel R, Sher I, Ben Ner D, et al. Chromatic multifocal pupillometer for objective perimetry and diagnosis of patients with retinitis pigmentosa. *Ophthalmology.* 2016;123:1898–1911.

30. Skaat A, Sher I, Kolker A, et al. Pupillometer-based objective chromatic perimetry in normal eyes and patients with retinal photoreceptor dystrophies. *Invest Ophthalmol Vis Sci.* 2013;54:2761–2770.